Acta Geologica Sinica (English Edition), 2021, 95(3): 937–945

Anisotropic Rock Poroelasticity Evolution in Ultra-low Permeability Sandstones under Pore Pressure, Confining Pressure, and Temperature: Experiments with Biot's Coefficient

DU Shuheng*

State Key Laboratory of Nonlinear Mechanics, Institute of Mechanics, Chinese Academy of Sciences, Beijing 100190, China

Abstract: This study aimed to show anisotropic poroelasticity evolution in ultra-low permeability reservoirs under pore pressure, confining pressure, and temperature. Several groups of experiments examining Biot's coefficient under different conditions were carried out. Results showed that Biot's coefficient decreased with increased pore pressure, and the variation trend is linear, but the decreasing rate is variable between materials. Biot's coefficient increased with increased confining pressure; the variation trend is linear, but the increasing rate varies by material as well. Generally, Biot's coefficient remains stable with increased temperature. Lithology, clay mineral content, particle arrangement, and pore arrangement showed impacts on Biot's coefficient. For strong hydrophilic clay minerals, expansion in water could result in a strong surface adsorption reaction, which could result in an increased fluid bulk modulus and higher Biot's coefficient. For skeleton minerals with strong lipophilicity, such as quartz and feldspar, increased oil saturation will also result in an adsorption reaction, leading to increased fluid bulk modulus and a higher Biot's coefficient. The study's conclusions provide evidence of poroelasticity evolution of ultra-low permeability and help the enhancing oil recovery (EOR) process.

Key words: Biot's coefficient, ultra-low permeability, pore pressure, confining pressure, temperature

Citation: Du, 2021. Anisotropic Rock Poroelasticity Evolution in Ultra-low Permeability Sandstones under Pore Pressure, Confining Pressure, and Temperature: Experiments with Biot's Coefficient. Acta Geologica Sinica (English Edition), 95(3): 937–945. DOI: 10.1111/1755-6724.13886

1 Introduction

The mechanical properties of rock are of great significance for oil and gas exploration, development and exploitation. In recent years, scholars and engineers pay more and more attention to using the mechanical properties of rock to find sweet spots and enhance oil recovery (Liu et al., 2016; Chen et al., 2017; Cao et al., 2018; Nguyen et al., 2018; Zhao et al., 2018)

The effective stress principle described by Terzahi (1923) pointed out that stress borne by underground rock can be placed in one of two categories: that borne by the rock skeleton is called effective stress, while that borne by pore fluid is called pore pressure. Biot (1944, 1955) thought seismic wave energy loss in formations could be due to the interaction between the viscous fluid and the solid skeleton. Biot's coefficient was proposed to quantitatively the characterize significance of the viscoelastic fluid. Geertsma et al. (1961), Nur et al. (1992, 1998) and Murphy et al. (1993) studied the relationship between Biot's coefficient and pure dry sandstone modulus through core testing. Zhang et al. (1996) measured Biot's coefficient via triaxial compression experiments and pointed out the significance of Biot's coefficient to horizontal stress calculation and fracturing design by deducing the theory formula. Ge et al. (2000) proposed a general predictive model of Biot's coefficient using theoretical derivation. Lu et al. (2005) put forward the equation between anisotropic Biot's coefficient rock damage by combining experimental and theoretical derivation methods, but did not put forward a quantitative characterization method for anisotropy. Ma et al. (2008) performed the experiment on selected sandstone samples formed in the Paleogene at the Jiyang Depression in order to study the influences of lithology and effective pressure on Biot's coefficient, but did not consider the factor of pore pressure change. Hu et al. (2009) studied the role Biot's coefficient plays in the case of marbles with cracks, pointing out the anisotropy of Biot's coefficient and its relationship with rock deformation, but not considering the influences of temperature. Alam et al. (2010) studied how different porosity reduction mechanisms change the strength of deep-sea carbonate-rich sediments and affect Biot's coefficient. Li et al. (2012) established an interpretation model for Biot's coefficient based on core test results using the generalized Usher model, but did not take anisotropy into account. Dou et al. (2012) deduced the relationship between the rock skeleton's coefficient, compressibility of the rock, and compressibility of rock pores through theoretical derivation, criticizing previous research that showed low-permeability reservoirs to have little stress sensitivity.

In short, many scholars have researched the role of Biot's coefficient in the behavior of numerous rock

* Corresponding author. E-mail: dushuheng@imech.ac.cn.

http://www.geojournals.cn/dzxbcn/ch/index.aspx; https://onlinelibrary.wiley.com/journal/17556724

materials, but no studies have focused on Biot's coefficient in relation to ultra-permeability sandstone or anisotropy thereof (Ciarletta et al., 2015; Du et al., 2015; Gao et al., 2015; Sarris et al., 2015; Tan et al., 2015). He et al. (2016) obtained Biot's coefficient after recording the variations of both the confining and pore pressures using a simplified measuring procedure. Ingraham et al. (2017) performed a series of constant mean stress (CMS) and constant shear stress (CSS) tests to investigate the evolution of permeability and Biot's coefficient at high mean stresses in a high porosity reservoir analog (Castlegate sandstone); CSS tests showed stabilization of Biot's coefficient after the application of shear stress. Rohan et al. (2020) considered acoustic waves in fluid-saturated periodic media with large contrasts in permeability and other poroelastic coefficients, and described the effective behavior through a model obtained via homogenization of the heterogeneous Biot continuum. Yuan et al. (2017) measured Biot's coefficient for samples of COx argillite cured at varying relative humidity levels.

Concerned about the state of such research at home and abroad, we identified three problems with previous study efforts (Ai et al., 2015; Bonomo et al., 2015; Dassanayake et al., 2015; Dobak et al., 2015; Rohan et al., 2020):

(1) Most rock measurements have been sampled from a single direction; they ought to be sampled from at least three directions (i.e., the *x, y* and *z* axes).

(2) Small experiments have been based on synchronous measurement of reservoir rocks' structure, composition, and so on; factors influencing anisotropy of Biot's coefficient go largely unexamined in such measurements.

(3) Up to the present, most studies and experiments have focused on dry samples, or on only one or two conditions such as confining pressure, pore pressure, temperature, etc. Small measurements were designed under specific underground reservoir conditions (temperature, confining pressure, pore pressure, or oil saturation level), so the results of most experiments could not describe reservoirs accurately.

For this paper, we selected typical reservoir rock samples from the study area in the Songliao Basin. We drilled three small samples from the *x*, *y*, and *z* axes in order to determine the parameters of rock mechanics under conditions of changing pore pressure, confining pressure or temperature to analyze the role and influence of Biot's coefficient with respect to microscopic anisotropy (Wu et al., 2014; El-Sayed et al., 2015; Garrido et al., 2015; Grassl et al., 2015; Lu et al., 2015).

2 Samples and Methods

Biot's coefficient is an important parameter in characterizing the poroelasticity of rocks, and is mainly used to determine the degree of influence of pore pressure on rock deformation (Xue et al., 2014; Wei et al., 2016; Fang et al., 2018). Its value range is between 0 and 1.

For the study, we used a servo rock mechanics triaxial stress test system (Fig. 1), which includes an axial pressure control system, pore pressure control system, confining pressure control system, and computer acquisition and control system. Confining pressure and pore pressure changes were recorded through the pressure sensor and pressure gauge. The system's computers automatically collected voltage signals via the sensors and converted them to force and displacement data for storage (Du et al., 2015).

Fig. 1. Servo rock mechanics triaxial stress test system (Du et al., 2015).

The confining pressure control system handled a maximum of 70 MPa; the pressure sensor and pressure gauge handled up to 40 MPa.

We selected typical reservoir rock samples, drilled small columns (diameter 25 mm, height 50mm) from each sample's *x*, *y*, and *z* axes (Fig. 2), and determined rock mechanics parameters under conditions of single changing factors for each sample. Basic information from this experimental process is shown in Suppl. Table 1.

3 Experimental Results

Biot's coefficient can represent poroelasticity well. The higher the Biot coefficient is, the bigger the stiffness of the pore is, the more difficult the pore is to be compressed. On the contrary, the lower the Biot coefficient, the smaller the stiffness of the pore is, the easier the pore is to be compressed (Tan et al., 2014; Yang et al., 2015; Luo et al., 2015; Pimienta et al., 2015; Straughan et al., 2018).

In order to explore anisotropic poroelasticity evolution in ultra-low permeability sandstones, we put samples from three groups (A, B, and C) into the triaxial test system for rock mechanics. We then changed the pore pressure, confining pressure, and temperature conditions separately, keeping the other factors under in-situ conditions. We

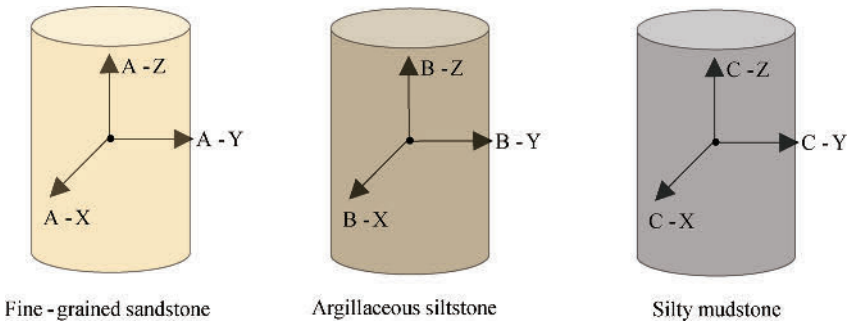

Fig. 2. Procedures for drilling rock samples from multiple directions.

determined Biot's coefficient under each set of conditions; measured results are shown in Figs. 3–5. A small part of the above experimental results are also used to study the crucial rock mechanics properties from other perspectives (Fang, 2016; Wang, 2016; Fang et al., 2018).

3.1 Pore pressure and poroelasticity

In any porous system subjected to an external load, the part of the load supported by the fluid in the pore is called pore pressure, and is one of the most important factors in petroleum exploration, development, and exploitation.

We kept the confining pressure, and temperature of all the samples under in-situ conditions, then changed the pore pressure from 4 MPa to 24 MPa or 26 MPa to determine the evolution of Biot's coefficient so that we could discover the impact mechanism between pore pressure and poroelasticity (Fig. 3 and Suppl. Tables 2–4).

Biot's coefficient decreased with increased pore pressure, and the variation trend is linear, but the decreasing rate varies by material. The decreasing rates for Biot's coefficient were highest in sample group A (fine-grained sandstone), moderate in C (silty mudstone), and lowest in B (argillaceous siltstone).

Each group of samples showed an interesting phenomenon: two curves were always close to each other; the third curve was always far from the other two, also showing significant anisotropy. For example, the A-X and A-Z curves are close in numerical value and much greater than A-Y; the C-X and C-Y curves are close in value and less than C-Z, etc. The difference between B-X, B-Y and B-Y is greatest, while the difference between A-X/Z and A-Y is the smallest. This mechanism is worth exploring.

3.2 Confining pressure and poroelasticity

Confining pressure refers to the pressure exerted on rock structures by surrounding rock structures. It is mainly caused by the weight of overlying rock, often called static rock pressure.

We kept the pore pressure and temperature of the three groups of samples under in-situ conditions, then changed the confining pressure from 10 MPa to 36 MPa to determine the evolution of Biot's coefficient so that we could discover the impact mechanism between confining pressure and poroelasticity (Fig. 4 and Suppl. Tables 5–7).

Biot's coefficient increased with increased confining pressure; the variation trend is linear, but the increasing rate varies by material. The increasing rates for Biot's coefficient were highest in sample group A (fine-grained sandstone), moderate in B (argillaceous sandstone), and lowest in C (silty mudstone).

The A/B sample groups showed an interesting phenomenon. The A-X and A-Z are close in numerical value and much greater than A-Y; the B-X and B-Z curves are much greater than B-Y but also distant from each other in value. The numerical difference between B-X, B-Y and B-Y is much greater than that between A-X/Z and A-Y.

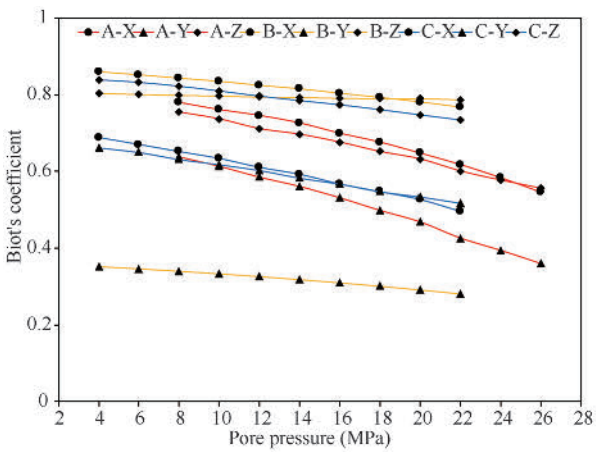

Fig. 3. Biot's coefficient determination for three groups under changing pore pressure conditions.

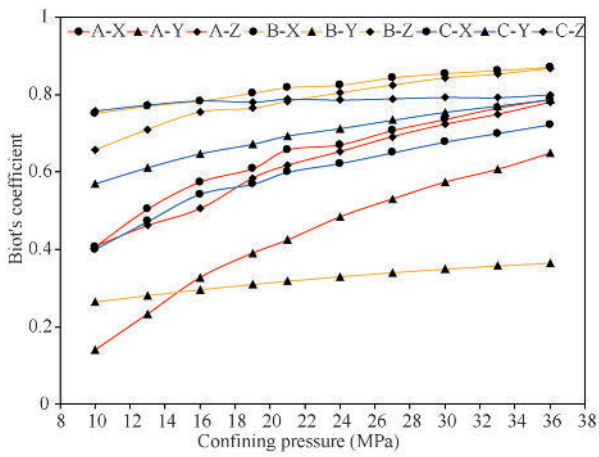

Fig. 4. Biot's coefficient determinations for three groups under changing confining pressure conditions.

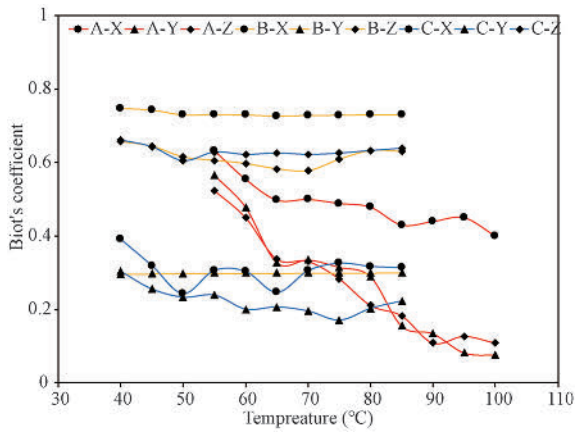

Fig. 5. Biot's coefficient determinations for three groups under changing temperature conditions.

For the C group, the distribution of the three curves is uniform. These values show a vast difference between the effects of confining pressure and those of pore pressure, and this mechanism is also worth exploring.

3.3 Temperature and poroelasticity

Temperature is a physical quantity that indicates the degree of heat or cold in a given object. Microscopically, it is the intensity of the thermal motion of the object molecule. Here, temperature mainly refers to the temperature of the environment in which rock samples are located.

We kept the pore pressure and confining pressure of the three groups of samples under in-situ conditions, then changed the temperature to determine the evolution of Biot's coefficient so that we could discover the impact mechanism between temperature and poroelasticity (Fig. 5 and Suppl. Tables 8–10).

Biot's coefficient for group A (fine-grained sandstone) samples decreased with increased temperature, but the coefficients for group B (argillaceous sandstone) and C (silty mudstone) samples remained stable with some fluctuation.

The A-Y and A-Z curves were close in numerical value and lower than A-X; B-X and B-Z were close in value and higher than B-Y; C-X and C-Y were close in value and far lower than C-Z.

4 Discussion

4.1 Pore pressure and confining pressure

As Biot's coefficient can indicate the poroelasticity of a material in a given cutting direction, we selected samples of fine-grained and argillaceous sandstone and cut six thin sections of each in order to explore the mechanism of anisotropic poroelasticity evolution in ultra-low permeability sandstone. The cutting steps for the six thin sections are shown in Fig. 6.

As can be seen in Figs. 7 and 8, the fine-grained and argillaceous sandstone samples contained a large amount of clay minerals. The presence of these minerals could easily lead to water sensitivity-causing chemical reactions in the process of water-flooding development, inevitably leading in turn to fluid entering and potentially altering the mechanical properties of essential skeleton materials. As this potential chain reaction illustrates, such factors as fluid properties and saturation affect Biot's coefficient throughout whole rock structures.

Rock particles mainly consisted of calcium feldspar and quartz. We put samples under a polarizing microscope (Figs. 7 and 8). We found that in A/B-X and A/B-Z, the

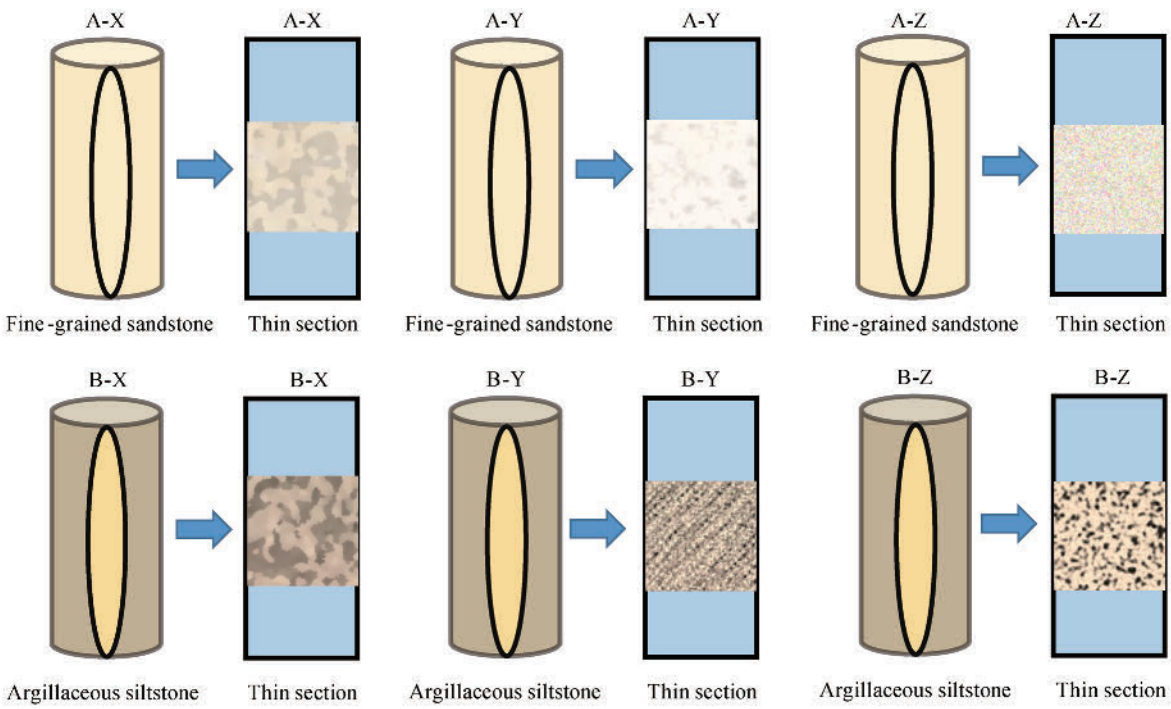

Fig. 6. Cutting methods for the thin sections of low-permeability sandstone.

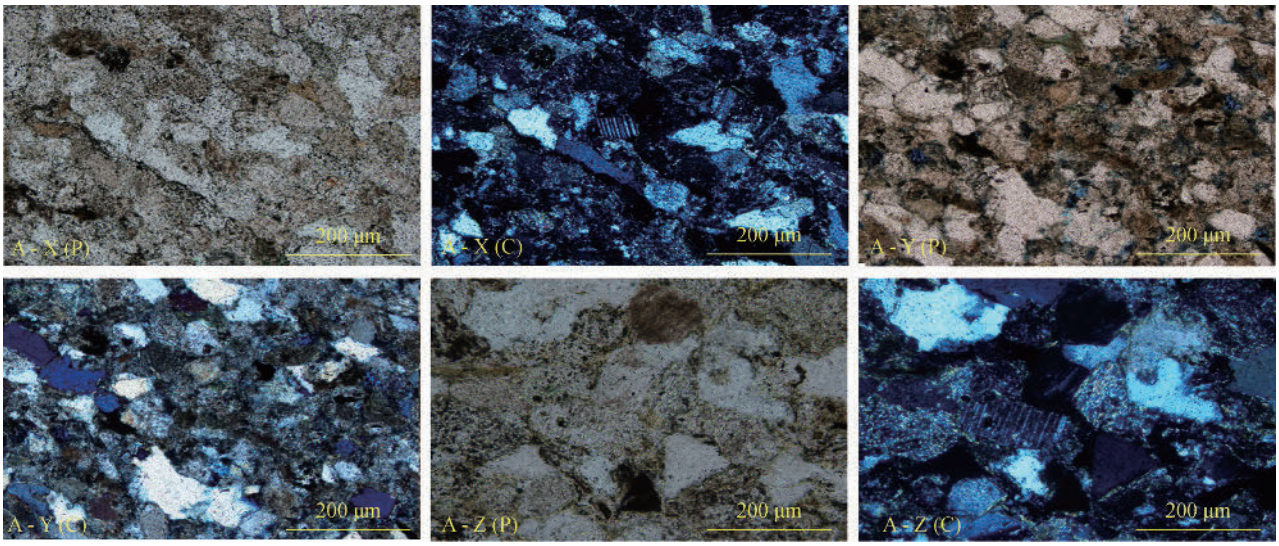

Fig. 7. Characteristics of horizontal and vertical rock slices from group A.
"C" indicates images taken under cross-polarized light (cpl); "P"indicates images taken under plane-polarized light (ppl).

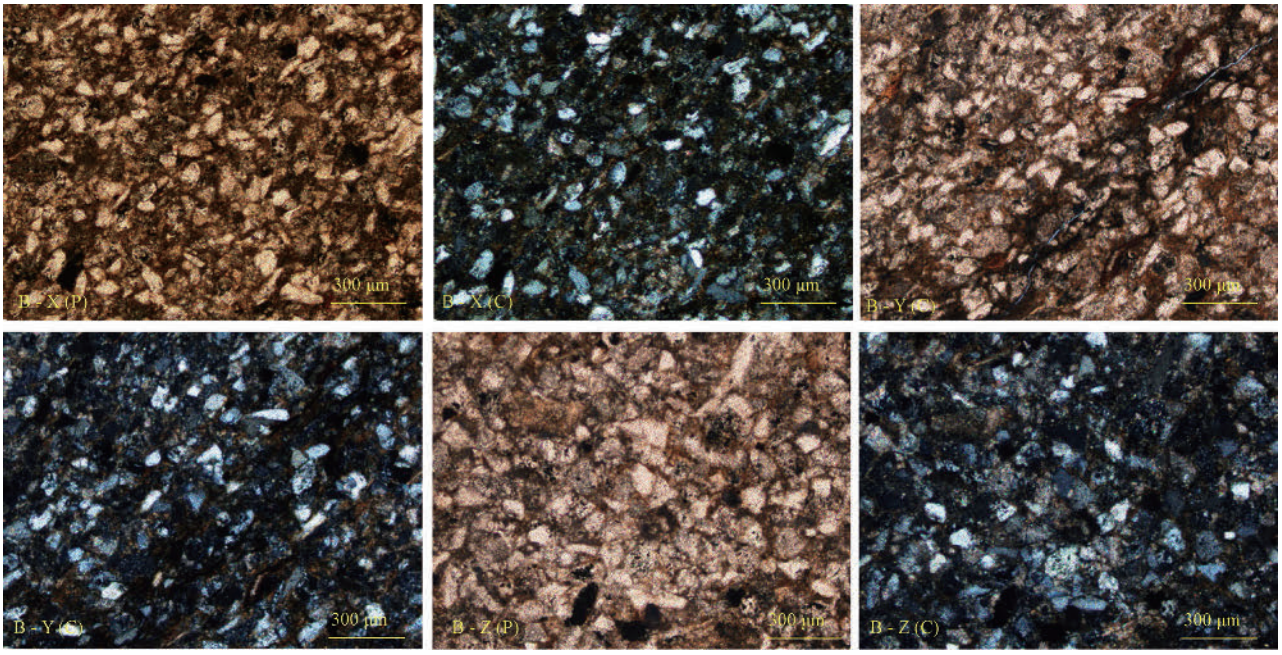

Fig. 8. Characteristics of horizontal and vertical rock slices from group B.
"C" indicates images taken under cross-polarized light (cpl); "P" indicates images taken under plane-polarized light (ppl).

directivity of the particle arrays was not strong; micro-fractures could be found easily; and inter-granular pore count and fluid content were high. Conversely, for A/B-Y, the directivity of the particle array was more pronounced; pores were more dispersed and the majority were "dead"; and fluid content was low. As a result of these differences, the absolute values of Biot's coefficient in A/B-X and A/B -Z were close and both larger than that of A/B-Y under conditions of changing pore and confining pressure.

Increased pore pressure or decreased confining pressure both directly led to difficulty of compression and corresponding decrease in fluid bulk modulus, so Biot's coefficient showed a trend of decline under these altered pressure conditions.

4.2 Temperature

When the temperature of the system increased, thermal expansion sometimes occurred, leading to increased pore pressure and corresponding decreases in fluid bulk modulus and Biot's coefficient. However, high temperature makes rock particles soft, increasing compression difficulty along with skeleton bulk modulus, so Biot's coefficient showed a trend of decline. Frankly speaking, this paper only provides possible explanations on above phenomenon, and the exact mechanism needs to be explored in the future research.

Consider the samples of fine-grained sandstone: at high temperatures, Biot's coefficient for "A-Y" was significantly reduced in value, dipping well below "A-X" (refer to Fig. 5).

As can be seen in Figs. 7 and 8, pores could not be found easily in A-Y from observation of rock slices. Intra-granular pores were given priority among pore types. Where mixed clay content is high, high temperature leads to inflation of pore fluid. This increases pore pressure, limiting the interface between fluid and particle, and could lead to fluid bulk modulus reduction, along with a drastic increase in the absolute value of Biot's coefficient for A-Y.

4.3 Application of anisotropic Biot's coefficient in hydraulic fracture prediction

The theoretical framework of mechanics is indispensable for the study of hydraulic fracturing process (Zhao，2016 and 2018). Prediction of fracture distribution in hydraulic fracturing is of great significance for enhancing oil and gas recovery (Chen et al., 2015; Moghadasi et al., 2019; Xu et al., 2019; Panja et al., 2020).

In order to explain why poroelasticity is of great significance to stress change, we have put the formula of total stress as following equation (1),

$$s = m(s_v - aD_{tv}\gamma_p)/(1-m) + aD_{tv}\gamma_p + \varepsilon_x E + s_t \quad (1)$$

where: "s_v" indicates overlying stress (MPa), "s" indicates the total stress (MPa), "m"-Poisson's ratio, "D_{tv}" indicates vertical depth of reservoir (m), "γ_{ob}" indicates the overlying stress gradient (MPa/m), "γ_p " indicates the pore pressure gradient (MPa/ m), "a" indicates the Biot's coefficient, "ε_x" indicates horizontal strain, "E" indicates Young's modulus (10^4 MPa), "s_t" indicates additional amount of tectonic stress, this value varies with depth it must be segmented into account. It can be seen from equation (1) that Biot's coefficient appears in two positions, so it will have a more important impact on stress value, and stress value is one of the core factors affecting fracture initiation and extension. Therefore, considering the change of Biot's coefficient is of great significance for the stimulation of low permeability reservoirs.

The heterogeneity of Biot's coefficient in main reservoir could have an important impact on the expansion of the artificial fracture in the process of hydraulic fracturing, which also directly related to the judgement of sweep volume and the effect of reservoir stimulation. Take the reservoir near to the study area, on the basis of using the experience of many modeling process, method of combining logging and sedimentary data was adopted, the fine reservoir geological model was set up (Fig. 9).

The specific process is as follows. Firstly, combining the data of core, multipole array acoustic logging (MAC), conventional logging, well models of physical properties and mechanical parameters were set up; Secondly, the cross-well models of the mechanical parameters of rock mass and physical properties were set up by the constrained interpolation of the sedimentary sand body model; Lastly, vector superposing was performed which consists gravity stress, tectonic stress, pore pressure model then the total stress model was established. In the study area, the direction of the maximum horizontal principal stress is 10 degree north by west. Because directions of confining pressure and pore pressure are both consistent with the radial direction of test samples, so Biot's coefficient of Z sample characterize the horizontal Biot's coefficient of the initial reservoir, and Biot's coefficient of X and Y characterize the vertical Biot's coefficient of the initial reservoir. Using the average value of X, Y to calculate the vertical Biot's coefficient and using the value of Z to calculate the horizontal Biot coefficient, so the three-dimensional horizontal and vertical Biot's coefficient model were established. (Fig. 9).

We predicted the artificial fracture of the specific reservoir in the "whole-fracture length" level instead of "half-fracture length" by innovative adopting the international advanced finite quantitative simulation software. In the predicting process, we choose three simulation methods to prove that considering heterogeneity of Biot's coefficient and dividing it into horizontal and vertical respectively is rather important to improve the predictive accuracy of fracture distribution. Three methods are explained as follows (a, b, and c):

(a) On the basis of the above models besides Biot coefficient, cut the profile models which pass through single-well respectively along the direction of maximum horizontal principal stress (10 degree north by west), import data of profile models into the fracturing simulation software. In the In the process of fracturing simulation, data of the horizontal and vertical Biot's coefficient are also important parameters which need to be provided. In this method, we used data of the logging curve to represent the whole profile. Namely, as to a specific depth value in a profile, data of horizontal and vertical Biot's coefficient don't change in the horizontal direction. They just change with depth values in the vertical direction.

(b) In addition to Biot coefficient, we adopted the model data of other attributes to import into the fracturing simulation software, arithmetic mean of horizontal and vertical Biot's coefficient were calculated, import the mean into fracturing simulation software, namely, in this method, we treated the horizontal and vertical Biot's coefficient are equal.

(c) All attributes data are imported into the fracturing simulation software by using the model data.

According to the engineering practice, fracturing operation parameters such as the sand content, sand fluid ratio and slurry rate etc. were set up. We got three different results of the artificial fracture distribution by using above three methods (Fig. 10)

As can be seen from the three simulation results (Fig. 10), the heterogeneity of Biot's coefficient will have large influence on the distribution law of fracture. In the first method, we suppose, as a specific depth value in a profile, data of horizontal and vertical Biot's coefficient don't change in the horizontal direction. Thus it led to the estimate result of the fracture distribution is too optimistic, the width of the value is generally bigger than the simulation results in the second and third method.

For the second simulation method, though it considered the fact that Biot's coefficient distribution is

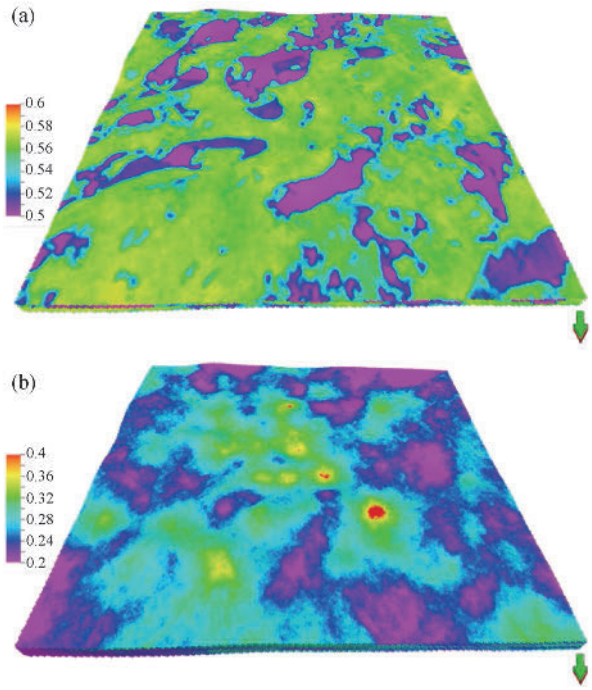

Fig. 9 Models of three-dimensional Biot's coefficient.
(a) Horizontal Biot's coefficient; (b) vertical Biot's coefficient

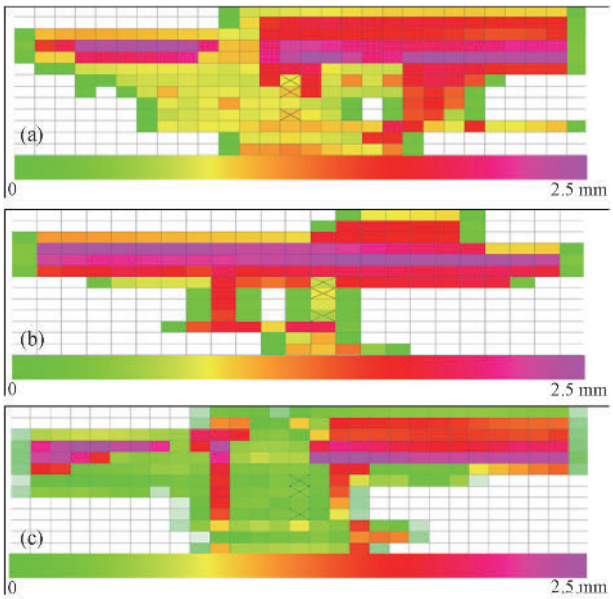

Fig. 10. Simulation results of fracture distribution by three methods respectively.
The black "X" symbols perforations, during the process of fracturing, the fracture extended away from wellbore, the horizontal grid length indicates the fracture length, the vertical grid length indicates the fracture height, the color of grid indicates fracture width, the step length of horizontal and vertical grid is 10 m, 2 m respectively.

heterogeneous, but it treated the horizontal and vertical Biot's coefficient as the same value. The simulation results showed that, fracture length is short near the perforation which indicates that sandstone reservoir near the perforation did not produce the fracture. Meanwhile, fracture near mudstone layer above perforation is long and the width values were bigger than which in sandstones, which is obviously far away from the geologic fact.

For the third simulation method, Biot's coefficient is divided into vertical and horizontal one, and the fact that Biot's coefficient distribution is heterogeneous is also be considered. Both two parameters were imported by using the model data. As can be seen from the simulation result, the average width value between which in the first and second method. According to the geological fact, the width value would change gradually at the fracture tip which could prove that the result calculated from the first method is better than which of the other two.

5 Conclusion

Lithology, clay mineral content, particle arrangement, and pore arrangement all have impacts on Biot's coefficient in ultra-permeable sandstone reservoirs.

Increased pore pressure and decreased confining pressure both lead directly to difficulty of compression, accompanied by decreased fluid bulk modulus and a trend of decline for Biot's coefficient.

When the temperature of the system is increased, thermal expansion can occur. This leads to increased pore pressure, accompanied by an increase in fluid bulk modulus and a decrease in Biot's coefficient; meanwhile, high temperatures may soften rock particles, increasing skeleton bulk modulus and creating a trend of decline for Biot's coefficient.

For strong hydrophilic clay minerals, expansion in water could result in a strong surface adsorption reaction, which could result in an increased fluid bulk modulus and higher Biot's coefficient. For skeleton minerals with strong lipophilicity, such as quartz and feldspar, increased oil saturation will also result in an adsorption reaction, leading to increased fluid bulk modulus and a higher Biot's coefficient.

As to the application of anisotropic Biot's coefficient in hydraulic fracture prediction, the Biot's coefficient would be one of the most important factor in hydraulic fracturing engineering.

Generally speaking, this paper is a case study, and the conclusion has its scope of application. The author of this paper also believes that some explanations of Biot's coefficient will be updated with the further study. In general, the Biot's coefficient related to the reservoir rocks is of great significance for the effective development of oil and gas.

Acknowledgments

This work was supported by PetroChina Innovation Foundation (Grant No.2019D-5007-0214).

Manuscript received Jan. 8, 2019
accepted Feb. 2, 2020
associate EIC: FEI Hongcai
edited by FEI Hongcai

Supplementary material in the article can be found online

at 10.1111/1755-6724.13886.

References

Ai, Z.Y., and Hu, Y.D., 2015. Multi–dimensional consolidation of layered poroelastic materials with anisotropic permeability and compressible fluid and solid constituents. Acta Geotechnica, 10(2): 263–273.

Alam, M.M., Borre, M.K., Fabricius, I.L., Hedegaard, K., Røgen, B., Hossain, Z., and Krogsbøll, A.S., 2010. Biot's coefficient as an indicator of strength and porosity reduction: Calcareous sediments from Kerguelen Plateau. Journal of Petroleum Science and Engineering, 70(3–4): 282–297.

Biot, M.A., 1941. General theory of three–dimensional consolidation. Journal of Application Physics, 12: 155–160.

Biot, M.A., 1955. Theory of elasticity and consolidation for a porous anisotropic solid. Journal of Application Physics, 26 (2): 182–185.

Bonomo, A.L., Chotiros, N.P., and Isakson, M.J., 2015. An assessment of the effective density fluid model for scattering from poroelastic sediments with inclusions. Journal of the Acoustical Society of America, 137(4): 2391.

Cao, R.H., Lin, H., and Cao, P., 2018. Strength and failure characteristics of brittle jointed rock–like specimens under uniaxial compression: Digital speckle technology and a particle mechanics approach. International Journal of Mining Science and Technology, 28(4): 669–677.

Chen, P., Ma, T.S., and Xia, H.Q., 2015. A collapse pressure prediction model for horizontal shale gas wells with multiple weak planes. Natural Gas Industry B, 2(1): 101–107.

Chen, Z.W., Shi, L., and Xiang, D.G., 2017. Mechanism of casing deformation in the Changning–Weiyuan national shale gas demonstration area and countermeasures. Natural Gas Industry B, 4(1): 1–6.

Ciarletta, P., and Fu, Y., 2015. A semi–analytical approach to Biot instability in a growing layer: Strain gradient correction, weakly non–linear analysis and imperfection sensitivity. International Journal of Non–Linear Mechanics, 75: 38–45.

Dassanayake, A.B.N., Fujii, Y., Fukuda, D., and Kodama, J.I., 2015. A new approach to evaluate effective stress coefficient for strength in Kimachi sandstone. Journal of Petroleum Science & Engineering, 131: 70–79.

Dobak, P., and Gaszynski, J., 2015. Evaluation of soil permeability from consolidation analysis based on Terzaghi's and Biot's theories. Geological Quarterly, 59(2): 373–381.

Dou, H.E., 2012. Discussion about rock compressibility and porosity applied in oilfield development. Xinjiang Petroleum Geology, 33(5): 617–622 (in Chinese with English abstract).

Du, S.H., Shi, Y.M., Bu, X.Q., Jin, W.Q., and Mu, G.Q., 2015. New expression of the changing stress field in lowpermeability reservoir and its application in secondary exploitation. Energy Exploration and Exploitation, 33(4): 491 – 514.

El-Sayed, M.F., Moussa, M.H. M., Hassan, A.A.A., and Hafez, N.M., 2015. Stability of viscoelastic fluid flowing through porous medium down non–uniformly heated inclined plane. Heat Transfer – Asian Research, 44(2): 109–132.

Fang, Y.Y., 2016. Establish a Biot coefficient calculating model containing the argillaceous matters and fluid types of sandstone reservoir (Master thesis). Beijing: Peking University, 1–137 (in Chinese with English abstract).

Fang, Y.Y., Shi, Y.M., Sheng, Y.S., and Zhang, Z.Q., 2018. Modeling of Biot's coefficient for a clay–bearing sandstone reservoir. Arabian Journal of Geosciences, 11(12): 1–17.

Gao, K., Van Dommelen, J.A.W., Göransson, P., and Geers, M.G.D., 2015. A homogenization approach for characterization of the fluidsolid coupling parameters in Biot's equations for acoustic poroelastic materials. Journal of Sound and Vibration, 351: 251–267.

Garrido, O.C., El Shawish, S., and Cizelj, L., 2015. Stress assessment in piping under synthetic thermal loads emulating turbulent fluid mixing. Nuclear Engineering and Design, 283: 114–130.

Ge, H.Q., Chen, Y., and Lin, Y.S., 2000. A general analytical model and geophysical interpretation of rock mechanics properties. Proceedings of the Sixth National Symposium on rock mechanics and Engineering. Beijing: Popular Science press, 251–255.

Geertsma, J., and Smit, D.C., 1961. Some aspects of elastic wave propagation in fluid saturated porous solid. Geophysics, 26(2): 169–181.

Grassl, P., Fahy, C., Gallipoli, D., and Wheeler, S.J., 2015. On a 2D hydromechanical lattice approach for modelling hydraulic fracture. Journal of the Mechanics and Physics of Solids, 75: 104–118.

He, J., Rui, Z.H., and Ling, K.G., 2016. A new method to determine Biot's coefficients of Bakken samples. Journal of Natural Gas Science and Engineering, 35: 259–264.

Hu, D.W., Zhou, H., Xie, S.Y., Zhang, K., Shao, J.F., and Feng, X.T., 2009. Study of Biot's coefficients of marble during plastic deformation phase. Rock and Soil Mechanics, 30(12): 3727– 3732 (in Chinese with English abstract).

Ingraham, M.D., Bauer, S.J., Issen, K.A., and Dewers, T.A., 2017. Evolution of permeability and Biot coefficient at high mean stresses in high porosity sandstone. International Journal of Rock Mechanics and Mining Sciences, 96: 1–10.

Li, Z.P., Zhou, W., Xie, R.C., and Shao, J., 2012. Preliminary study on non–linear interpretation of Biot's coefficient of rock and its application on the analysis of wellbore stability. Oil Drilling & Production Technology, 34(1): 39–42 (in Chinese with English abstract).

Liu, C., Xue, J.H., Yu, G.F., and Cheng X.Y., 2016. Fractal characterization for the mining crack evolution process of overlying strata based on microseismic monitoring technology. International Journal of Mining Science and Technology, 26(2): 295–299.

Lu, Y.F., Zhou, S.P., Tian, B., and Shao, J.F., 2005. Energy principle of rock and water interaction and Biot's coefficient. Rock and Soil Mechanics, 26(S2): 69–72 (in Chinese with English abstract).

Lu, Y.L., and Wang, L.G., 2015. Numerical simulation of mining -induced fracture evolution and water flow in coal seam floor above a confined aquifer. Computers and Geotechnics, 67: 157–171.

Luo, X., Were, P., Liu, J.F., and Hou, Z.M., 2015. Estimation of Biot's effective stress coefficient from well logs. Environmental Earth Sciences, 73(11): 7019–7028.

Ma, Z.G., 2008. Experimental investigation into Biot's coefficient and rock elastic moduli. Oil and Gas Geology, 29 (01): 135– 140 (in Chinese with English abstract).

Moghadasi, R., Rostami, A., and Hemmati–Sarapardeh A., 2019. Application of nanofluids for treating fines migration during hydraulic fracturing: Experimental study and mechanistic understanding. Advances in Geo–Energy Research, 3(2): 198–206.

Murphy, W., Reischer, A., and Hsu, K., 1993. Modules decomposition of compressional and shear velocity in sand bodies. Geophysics, 58(2): 227–239.

Nguyen, T.S., 2018. Thermo–hydro–mechanical–chemical processes in geological disposal of radioactive waste–An example of regulatory research. Advances in Geo–Energy Research, 2(2): 173–189.

Nur, A., 1992. Critical porosity and the seismic velocity in rocks. EOS Trans Am Geophys Union, 73: 43–66.

Nur, A., Mavko, G., Dvorkin, J., and Galmudi, D., 1998. Critical porosity: A key to relating physical properties to porosity in rock. The Leading Edge, 17(2): 357–362.

Panja, P., Velasco, R., and Deo, M., 2020. Understanding and modeling of gas–condensate flow in porous media. Advances in Geo–Energy Research, 4(2): 173–186.

Pimienta, L., Fortin, J., and Guéguen, Y., 2015. Bulk modulus dispersion and attenuation in sandstones. Geophysics, 80(2): D111–D127.

Rohan, E., Nguyen, V.H., and Naili, S., 2020. Numerical modelling of waves in double–porosity Biot medium. Computers and Structures, 232: 105849.

Sarris, E., and Papanastasiou, P., 2015. The influence of pumping parameters in fluid–driven fractures in weak porous formations. International Journal for Numerical and Analytical Methods in Geomechanics, 39(6): 635–654.

Straughan, B., and Tibullo, V., 2018. Thermal effects on nonlinear acceleration waves in the Biot theory of porous media. Mechanics Research Communications, 94: 70–73.
Tan, X., and Konietzky, H., 2014. Numerical study of variation in Biot's coefficient with respect to microstructure of rocks. Tectonophysics, 610: 159–171.
Tan, X., Konietzky, H., and Frühwirt, T., 2015. Experimental and numerical study on evolution of Biot's coefficient during failure process for brittle rocks. Rock Mechanics and Rock Engineering, 48(3): 1289–1296.
Terzaghi, K.V., 1923. Die Berechnung der Durchassigkeitsziffer des Tones aus dem Verlauf der hydrodynamischen Spannungserscheinungen. Akademie der Wissenschaften in Wien. Sitzungsberichte. 11: 105–124.
Wang, L., 2016. Hydraulic fracturing simulation based on the heterogeneous rock mechanics model (Ph.D. thesis). Beijing: Peking University, 1–137 (in Chinese with English abstract).
Wei, J.P., Li, B., Wang, K., and Sun, D.H., 2016. 3D numerical simulation of boreholes for gas drainage based on the pore–fracture dual media. International Journal of Mining Science and Technology, 26(4): 739–744.
Wu, G.C., Wu, J.L., and Zong, Z.Y., 2014. The attenuation of P wave in a periodic layered porous media containing cracks. Chinese Journal of Geophysics, 57(8): 2666–2677 (in Chinese with English abstract).
Xu, H.L., Kong, W.Y., and Yang, F.Q., 2019. Decomposition characteristics of natural gas hydrates in hydraulic lifting pipelines. Natural Gas Industry B, 6(2): 159–167.
Xue, S., Yuan, L., Xie, J., and Wang, Y.C., 2014. Advances in gas content based on outburst control technology in Huainan, China. International Journal of Mining Science and Technology, 24(3): 385–389.
Yang, S.P., Fang, X.Q., and Liu, J.X., 2015. Vibration prediction of water–saturated poroelastic ground induced by high speed train with sleeper effect. Applied Mathematical Modeling, 39 (12): 3331–3340.
Yuan, H.F, Agostini, F., Duan, Z.B., Skoczylas, F., and Talandier, J., 2017. Measurement of Biot's coefficient for COx argillite using gas pressure technique. International Journal of Rock Mechanics and Mining Sciences, 92: 72–80.
Zhang, B.P., Shen, W.B., and Shan, W.W., 1996. Applications of elastic modulus and Biot's coefficient of rock in fracturing design. Oil Drilling and Production Technology, 18(3): 60–65 (in Chinese with English abstract).
Zhao, J.Z., Ren, L., Shen, C., and Li, Y.M., 2018. Latest research progresses in network fracturing theories and technologies for shale gas reservoirs. Natural Gas Industry B, 5(5): 533–546.
Zhao, Y.P., 2016. Modern Continuum Mechanics. Beijing: Science Press, 1–553 (in Chinese).
Zhao, Y.P., 2018. Lectures on Mechanics. Beijing: Science Press, 1–385 (in Chinese).

About the first and corresponding author

DU Shuheng is an assistant professor at State Key Laboratory of Nonlinear Mechanics, Institute of Mechanics, Chinese Academy of Sciences. He received his B.A. in China University of Geosciences in 2013 and Ph.D. in Peking University in 2018. His current research interest is focused on unconventional hydrocarbon geology and mechanics. E-mail: dushuheng@imech.ac.cn.